The effect of magnetization orientation on the optical and magneto-optical properties of metals

1992 J. Phys.: Condens. Matter 4 1299

(http://iopscience.iop.org/0953-8984/4/5/010)

J. Phys.: Condens. Matter 4 (1992) 1299–1310. Printed in the UK

The effect of magnetization orientation on the optical and magneto-optical properties of metals

S V Halilov†
Kurchatov Institute of Atomic Energy, 123182, Moscow, USSR

Received 26 July 1991

Abstract. Analytical and numerical investigations are carried out to reveal the frequency and magnetization orientation dependences of the conductivity tensor components. Analysis of the perturbatively obtained expressions shows that the peculiarities of the tensor components that are even in magnetization are immediately related with the spin-flip transitions. The corresponding identification of the peculiarities of the orientation magneto-optical Kerr effect can allow one to extract the magnitude of an exchange splitting from experimental data. The results of application to Ni are presented.

1. Introduction

Recent first-principles calculations [1, 2] of the magnetocrystalline anisotropy energy of ferromagnetic metals indicate the need for further investigation of the effect of magnetization orientation on electronic properties. It can be assumed that the existing disagreement between theory and experiment as regards the energy changes resulting from changes in the direction of magnetization is due to insufficient accuracy of the present methods, which serve as a basis of numerical band calculations. In crystals with high symmetry, the effect of the magnetic anisotropy on total electron energy is of rather high order in the magnetization and relativistic terms compared with such phenomena as magneto-optical effects [3]. Furthermore, the effects of lattice distortion caused by magnetostriction and other similar effects, which are also connected with relativity, may prove to be useful in describing magnetic anisotropy energetics.

Probably, one of the most suitable macroscopic quantities is the optical conductivity tensor, which is not strongly sensitive to the accuracy of the present methods and by which the usual optical and magneto-optical properties are described. In general, the dissipation of light in a ferromagnet is described by both the diagonal and non-diagonal components of the conductivity tensor $\sigma_{\alpha\beta}(\omega)$ (see e.g. [3]) and depends on the magnetization (M) orientation.

In this paper the manifestation of the orientation effect in magneto-optics is investigated by the perturbation method with both the exchange splitting and spin–orbit (SO) coupling considered on an equal footing. An expression for the component of the tensor including only odd powers of the magnetization was first obtained by Argyres [4] for the

† Present address: Theoretische Festkörperphysik, Universität Duisburg-GH, W-4100 Duisburg, Federal Republic of Germany.

0953-8984/92/051299 + 12 $04.50

direction $M \| [0\,0\,1]$. The case of arbitrary orientation of M and both odd and even M components of the tensor in question are the subjects considered in the present paper.

The present paper is organized as follows. In section 2 a short review of the theoretical results on optics and magneto-optics is presented. Section 3 contains the perturbative expressions for the conductivity tensor obtained in the framework of the local spin-density approximation (LSDA). On the basis of these expressions, the angle and frequency dependences of both odd and even M components of $\sigma_{\alpha\beta}(\omega)$ are analysed. The relations between the conductivity tensor components and macroscopic magneto-optical effects for arbitrary magnetization direction are considered in section 4. Section 5 is devoted to the numerical calculations of the optical and magneto-optical characteristics of Ni (FCC) for different orientations of M. These calculations confirm the general expressions obtained perturbatively and allow comparison with the experimental data. Finally, in section 6, the concluding remarks and a summary are presented.

2. Conductivity tensor and light dissipation

Let us concentrate on those components of the conductivity tensor that describe light dissipation in a ferromagnet for a given orientation of M. What gives a contribution to light dissipation in conventional optics is, as is well known, $\mathrm{Re}\,\sigma_{\alpha\alpha}(\omega)$ for an arbitrary direction of M. Further, only the non-diagonal tensor components will be considered, with the exception of special cases.

Generally, tensor $\sigma_{\alpha\beta}(\omega)$ can be divided into two contributions, $\sigma^{s}_{\alpha\beta}(\omega)$ and $\sigma^{a}_{\alpha\beta}(\omega)$, which contain the odd and even powers of M, respectively:

$$\sigma_{\alpha\beta}(\omega) = \tfrac{1}{2}[\sigma_{\alpha\beta}(\omega) + \sigma_{\beta\alpha}(\omega)] + \tfrac{1}{2}[\sigma_{\alpha\beta}(\omega) - \sigma_{\beta\alpha}(\omega)] \equiv \sigma^{s}_{\alpha\beta}(\omega) + \sigma^{a}_{\alpha\beta}(\omega). \tag{1}$$

In equation (1), $\sigma^{s}_{\alpha\beta}(\omega)$ is symmetric and $\sigma^{a}_{\alpha\beta}(\omega)$ is antisymmetric with respect to the transposition $x \leftrightarrow y$. The contribution of the non-diagonal tensor components to light dissipation can be written in terms of the electric field complex intensity E as follows:

$$\begin{aligned} Q = (1/4\pi)\langle E\,\partial D/\partial t\rangle &= \tfrac{1}{2}\sum_{k\neq i} \mathrm{Re}\,\tfrac{1}{2}(\sigma_{ik}\langle E_i^* E_k\rangle + \sigma_{ki}\langle E_k^* E_i\rangle) \\ &= \sum_{k\neq i} [\tfrac{1}{2}\,\mathrm{Re}(\sigma_{ik} + \sigma_{ki})\,\mathrm{Re}\langle E_i^* E_k\rangle + \tfrac{1}{2}\,\mathrm{Im}(\sigma_{ki} - \sigma_{ik})\,\mathrm{Im}\langle E_i^* E_k\rangle]. \end{aligned} \tag{2}$$

This means that light dissipation for an arbitrary orientation of M is described by the antisymmetric (with respect to $\alpha \leftrightarrow \beta$) component $\frac{1}{2}\,\mathrm{Im}(\sigma_{\beta\alpha} - \sigma_{\alpha\beta})$ responsible for the linear magneto-optical effects and symmetric component $\frac{1}{2}\,\mathrm{Re}(\sigma_{\alpha\beta} + \sigma_{\beta\alpha})$ responsible for even magneto-optical effects.

The formulae for antisymmetric and symmetric tensor components can be easily derived from the general expressions based on Kubo's [5] formula for linear response:

$$\mathrm{Im}\,\sigma^{a}_{\alpha\beta}(\omega) = \frac{\pi e}{2m\omega}\sum_{k\lambda\lambda'} \delta(\hbar\omega - E_{\lambda,\lambda'}(k)) f_{k\lambda}(f_{k\lambda} - f_{k\lambda'})\,\mathrm{Im}[j_{\alpha}^{\lambda\lambda'}(k) j_{\beta}^{\lambda'\lambda}(k)] \tag{3}$$

and the same expression for $\mathrm{Re}\,\sigma^{s}_{\alpha\beta}(\omega)$ is obtained by substitution $\mathrm{Im} \leftrightarrow \mathrm{Re}$ in formula (3). The notations in equation (3) are as follows: $j_{\alpha}^{\lambda\lambda'}(k)$ are the current density operator matrix elements

$$j_{\alpha}^{\lambda\lambda'}(k) = (e/m)\langle \psi_{k\lambda}|\hat{p}_{\alpha} + (e\hbar/4mc^2)[\sigma \times \nabla v(r)]|\psi_{k\lambda'}\rangle \tag{4}$$

λ is the electron state, $E_{\lambda,\lambda'} \equiv E_{k\lambda} - E_{k\lambda'}$ and $f_{k\lambda}$ is the Fermi–Dirac function. To evaluate

expression (3), eigenstates and wavefunctions were derived from the Kohn–Sham equation including relativistic effects in first order of v^2/c^2 and the Zeeman term for arbitrary magnetization orientation:

$$[-(\hbar^2/2m)\nabla^2 + \nu(\boldsymbol{r}) + h_{so} + h_{zm}]\psi_{k\lambda}(\boldsymbol{r}) = E_{k\lambda}\psi_{k\lambda} \tag{5}$$

where $\nu(\boldsymbol{r})$ is the Hartree, electron–nuclear Coulomb and exchange–correlation contributions to the effective one-particle potential, h_{so} and h_{zm} are spin–orbit and Zeeman terms respectively:

$$\begin{aligned} h_{so} &= \xi(r)\boldsymbol{\sigma}\cdot\boldsymbol{l} = \xi(r)\tfrac{1}{2}\begin{pmatrix} \hat{l}_z & \hat{l}_- \\ \hat{l}_+ & -\hat{l}_z \end{pmatrix} \\ h_{zm} &= \Delta\nu(r)\bar{\sigma} = \Delta\nu(r)\begin{pmatrix} \cos\theta & \mathrm{e}^{-\mathrm{i}\varphi}\sin\theta \\ \mathrm{e}^{\mathrm{i}\varphi}\sin\theta & -\cos\theta \end{pmatrix} \\ \xi(r) &\equiv \frac{1}{2m^2c^2}\frac{1}{r}\frac{\partial\nu(t)}{\partial r} \qquad \Delta\nu(r) \equiv \tfrac{1}{2}\left(\frac{\delta E_{xc}[\hat{\rho}]}{\delta\rho_1} - \frac{\delta E_{xc}[\hat{\rho}]}{\delta\rho_2}\right) \end{aligned} \tag{6}$$

E_{xc} is the exchange–correlation energy, ρ_i are the diagonal elements of the density matrix $\hat{\rho}$, σ denotes the Pauli matrices, $\hat{l}$ is the angular momentum operator, and $\bar{\sigma}$ is the σ_z Pauli matrix rotated by the spin-1/2 rotation matrix diagonalizing the density matrix (see e.g. [6]). Potential magnetic and spin–orbit parameters are $\Delta\nu$ and $\xi(r)$, respectively. The orientation of the magnetization with respect to the crystallographic axes is set up by the spherical angles θ, φ. Numerical integration of equation (5) was performed self-consistently by the linear muffin-tin orbitals (LMTO) method [7], which includes combined correction terms.

Some remarks concerning the numerical integration over $\boldsymbol{k}$ in equation (3) should be made. To integrate over the irreducible part of the Brillouin zone (IBZ), the following condition should be taken into account:

$$\sum_{BZ} f(\boldsymbol{k}) = \sum_{IBZ}\frac{1}{N_g}\sum_{\hat{g}}\hat{g}f(\boldsymbol{k}) \tag{7}$$

where $\hat{g}$ are the elements of the magnetic point group, N_g is the group order and $f(\boldsymbol{k})$ is the integrand.

3. Perturbative expressions for tensor components

It can be useful to obtain the obvious frequency-dependent expressions with the extracted orientational dependence to analyse and treat the frequency behaviour and peculiarities of the tensor non-diagonal components versus the magnetization orientation. The perturbative derivation of these expressions is the point at issue of the present section.

The perturbative wavefunction can be written in the second order of h_{so} in the usual way:

$$\begin{aligned} \hat{\psi}_{\gamma s} = \hat{\psi}^0_{\gamma s} &+ \sum_{m\sigma}{}' \frac{\langle m\sigma|h_{so}|\gamma s\rangle}{E_{\gamma s,m\sigma}}\hat{\psi}^0_{m\sigma} + \sum_{m\sigma}{}'\sum_{m'\sigma'}{}' \frac{\langle m\sigma|h_{so}|m'\sigma'\rangle\langle m'\sigma'|h_{so}|\gamma s\rangle}{E_{\gamma s,m'\sigma'}E_{\gamma s,m\sigma}}\hat{\psi}^0_{m\sigma} \\ &- \sum_{m\sigma}{}' \frac{\langle\gamma s|h_{so}|\gamma s\rangle\langle m\sigma|h_{so}|\gamma s\rangle}{E^2_{\gamma s,m\sigma}}\hat{\psi}^0_{m\sigma} - \sum_{m\sigma}{}' \frac{|\langle m\sigma|h_{so}|\gamma s\rangle|^2}{E^2_{\gamma s,m\sigma}}\hat{\psi}^0_{\gamma s} \end{aligned} \tag{8}$$

where $\hat{\psi}^0_{\gamma s}$ is the spinor (γ and s are the band and spin indices, respectively) obeying equation (5) with h_{so} omitted. The spinors $\hat{\psi}^0_{\gamma s}$ can be derived in the first order of h_{zm} from the corresponding secular equation as the linear combination of the spin-restricted and non-relativistic wavefunctions φ^0_γ (spinors $\hat{\varphi}^0_\gamma$):

$$\hat{\psi}^0_{\gamma s} = \frac{1}{\sqrt{2}} \begin{pmatrix} \exp(-i\varphi/2) & (1 \pm \cos\theta)^{1/2} \\ \pm\exp(i\varphi/2) & (1 \mp \cos\theta)^{1/2} \end{pmatrix} \varphi^0_\gamma \qquad s = 1, 2. \tag{9}$$

The one-particle energy spectrum does not depend on the magnetization orientation in the first order of h_{zm} and h_{so}:

$$\begin{aligned} E_{\gamma s} &= E^0_\gamma + \langle \hat{\varphi}_{\gamma s} | h_{zm} | \hat{\varphi}_{\gamma s} \rangle + \langle \hat{\varphi}_{\gamma s} | h_{so} | \hat{\varphi}_{\gamma s} \rangle \\ &\simeq E^0_\gamma \mp \langle \varphi_\gamma | \Delta\nu | \varphi_\gamma \rangle \qquad s = 1, 2. \end{aligned} \tag{10}$$

Then the expressions in question can be obtained by the substitution of formulae (8)–(10) into equation (3) for $\mathrm{Im}\,\sigma^a_{\alpha\beta}(\omega)$ and $\mathrm{Re}\,\sigma^s_{\alpha\beta}(\omega)$. To get clearer formulae for the tensor components considered, it is necessary to take into account the point-group restrictions on the terms that arise as a result of the above-mentioned substitution. For cubic crystals, such manipulations lead to the following final expressions for the antisymmetric (odd in $\boldsymbol{M}$) and symmetric (even in $\boldsymbol{M}$) non-diagonal tensor components:

$$\begin{aligned} \mathrm{Im}\,\sigma^a_{xy}(\omega) \simeq \frac{\pi e^2}{2m^2\omega} \sum_{k\gamma\gamma'}{}' \sum_m{}' \{ & [F^{11}_{m\gamma'}(\boldsymbol{k}, \theta, \varphi)(p^{\gamma m}_x p^{\gamma'\gamma}_y - p^{\gamma m}_y p^{\gamma'\gamma}_x) \\ & + F^{11*}_{m\gamma}(\boldsymbol{k}, \theta, \varphi)(p^{m\gamma'}_x p^{\gamma'\gamma}_y - p^{m\gamma'}_y p^{\gamma'\gamma}_x)] \\ & \times \delta(\hbar\omega - E_{\gamma' 1,\gamma 1}) f_{k\gamma 1}(f_{k\gamma 1} - f_{k\gamma' 1}) - \mathrm{terms}(1 \leftrightarrow 2)\} \end{aligned} \tag{11}$$

with

$$F^{\sigma\sigma}_{m\gamma}(\boldsymbol{k}, \theta, \varphi) = -i[\langle \xi l_z \rangle_{m\gamma} \cos\theta + (1/\sqrt{2})(\langle \xi l_x \rangle_{m\gamma} + \langle \xi l_y \rangle_{m\gamma}) \sin(\varphi + \pi/4) \sin\theta]/E_{m\sigma,\gamma\sigma}$$

and

$$\begin{aligned} \mathrm{Re}\,\sigma^s_{\alpha\beta}(\omega) \simeq \frac{\pi e^2}{2m^2\omega} \sum_{k\gamma\gamma'}{}' \sum_\sigma [& A^{\gamma\gamma'\cdot\sigma}_{\alpha\beta}(\boldsymbol{k}, \theta, \varphi) \delta(\hbar\omega - E_{\gamma'\sigma,\gamma\sigma}) f_{k\gamma\sigma}(f_{k\gamma\sigma} - f_{k\gamma'\sigma}) \\ & + B^{\gamma\gamma'\cdot\sigma}_{\alpha\beta}(\boldsymbol{k}, \theta, \varphi) \delta(\hbar\omega - E_{\gamma'\sigma,\gamma\bar{\sigma}}) f_{k\gamma\sigma}(f_{k\gamma\sigma} - f_{k\gamma'\bar{\sigma}})] \end{aligned} \tag{12}$$

where the spin-degenerate and non-relativistic wavefunctions are used for matrix elements, $\sigma(\bar{\sigma}) = 1(2)$, $2(1)$ denote the spin projection numbers, $E_{\gamma'\sigma,\gamma\bar{\sigma}} \equiv E_{\gamma'\sigma}(\boldsymbol{k}) - E_{\gamma\bar{\sigma}}(\boldsymbol{k})$, and the expressions for $A^{\gamma\gamma'\cdot\sigma}_{\alpha\beta}(\boldsymbol{k}, \theta, \varphi)$ and $B^{\gamma\gamma'\cdot\sigma}_{\alpha\beta}(\boldsymbol{k}, \theta, \varphi)$ are presented in the appendix. There are some simplifying assumptions, which result in the obtained formulae (11) and (12). These are the reality of the momentum matrix elements and imaginarity of the spin–orbit coupling matrix elements in the presence of space inversion. Moreover, the presence of fourth-order rotation axes $\hat{\delta}_{4x}$, $\hat{\delta}_{4y}$, $\hat{\delta}_{4z}$ is implied for the crystallographic point group to obtain equation (12) (such a situation is realized for example in cubic crystals). Expression (11) is valid for crystals with arbitrary symmetry including space inversion. It is obvious from equations (11) and (12) that $\mathrm{Im}\,\sigma^a_{xy}$ and $\mathrm{Re}\,\sigma^s_{xy}$ are really antisymmetric and symmetric with respect to the transposition $x \leftrightarrow y$, respectively.

For cubic crystals the symmetric restrictions induced by the mirror operation $\hat{\sigma}_z$ lead to a simple dependence of the antisymmetric component $\mathrm{Im}\,\sigma^{a}_{xy}(\omega)$ on the magnetization orientation:

$$\mathrm{Im}\,\sigma^{a[\theta,\varphi]}_{xy}(\omega) \simeq \mathrm{Im}\,\sigma^{a[001]}_{xy}(\omega)\cos\theta. \tag{13}$$

It should be noted that the derived expression (11) for the antisymmetric tensor component $\mathrm{Im}\,\sigma^{a}_{xy}$ corresponds to the first order in $(\bar{h}_{so}/\bar{E}_{\lambda\lambda'})$ of the series expansion, where $\bar{h}_{so}$ and $\bar{E}_{\lambda\lambda'}$ are the averaged spin–orbit splitting and distance between the nearest valence states, respectively. The formula (12) obtained for the symmetric tensor component $\mathrm{Re}\,\sigma^{s}_{xy}$ corresponds to the second order in $(\bar{h}_{so}/\bar{E}_{\lambda\lambda'})$ of the series expansion. At low frequency $\omega \sim \bar{h}_{so}/\hbar$, hybridization between the states due to the spin–orbit coupling should be taken into account (see [8], where the corresponding analytical expressions for θ, $\varphi = 0$, i.e. for $\boldsymbol{M}\|[001]$, are reproduced). Generally speaking, the discussed formulae (11) and (12) are invalid at $\omega \sim \bar{h}_{so}/\hbar$.

One of the most characteristic features of the tensor components in question consists of the difference between interband mechanisms forming antisymmetric and symmetric components. As follows from equation (11), the antisymmetric component $\mathrm{Im}\,\sigma^{a}_{xy}(\omega)$ can be roughly represented as the difference between the interband spin-up and spin-down transitions. In contrast, the symmetric component $\mathrm{Re}\,\sigma^{s}_{xy}$ is formed by the spin-flip transitions, as well as the usual interband transitions between the states with the same spin projections.

It should be noted that the effective one-particle potential $v(r)$ used in the wave equation (5) is assumed to be spherical on each site. Such an assumption simplifies the calculations in question but leads to a well known problem concerning the sharp spin orientation degeneracy removal induced by the infinitely small magnetic field in the spherically symmetric electron system (see e.g. [9–11]). An additional simplification used for calculations consists of the independence of the spin rotation matrix at a point inside the given atomic sphere. Moreover, in the framework of the density-functional formalism, the spinors used in the perturbative expressions discussed have to be self-consistent. However, the perturbative expressions obtained above seem to be convenient for magnetic systems with well localized magnetic moment in which the amplitude of the spontaneous magnetic moment is not practically dependent on the magnetization orientation. To avoid these difficulties, the natural anisotropic terms fixing the spin orientation in the absence of the magnetic field should be added to the Hamiltonian. For instance, the more realistic non-spherical effective potential can probably remove this problem, which however is beyond the scope of the present paper.

In the small-magnetization limit the expression for $\mathrm{Re}\,\sigma^{s}_{\alpha\beta}$ can be reproduced as follows:

$$\begin{aligned}\mathrm{Re}\,\sigma^{s}_{xy}(\omega) \sim \sum_{k\gamma\gamma'} \sin(2\varphi)\sin^2\theta\,\{a^{\gamma\gamma'}_{xy}[f_{\gamma 1}(1-f_{\gamma' 1})\delta(\hbar\omega - E_{\gamma' 1\gamma 1})\\ - f_{\gamma 2}(1-f_{\gamma' 2})\delta(\hbar\omega - E_{\gamma' 2\gamma 2})] + b^{\gamma\gamma'}_{xy}[f_{\gamma 1}(1-f_{\gamma' 2})\delta(\hbar\omega - E_{\gamma' 2\gamma 1})\\ - f_{\gamma 2}(1-f_{\gamma' 1})\delta(\hbar\omega - E_{\gamma' 1\gamma 2})]\}\,2\overline{\Delta\nu}\end{aligned} \tag{14}$$

$$\begin{aligned}\mathrm{Re}\,\sigma^{s}_{\alpha\beta}(\omega) \sim \sum_{k\gamma\gamma'} [\{a^{\gamma\gamma'}_{\alpha\beta}(\theta,\varphi)[f_{\gamma 1}(1-f_{\gamma' 1})\delta(\hbar\omega - E_{\gamma' 1\gamma 1})\\ - f_{\gamma 2}(1-f_{\gamma' 2})\delta(\hbar\omega - E_{\gamma' 2\gamma 2})]\\ + b^{\gamma\gamma'}_{\alpha\beta}(\theta,\varphi)[f_{\gamma 1}(1-f_{\gamma' 2})\delta(\hbar\omega - E_{\gamma' 2\gamma 1})\end{aligned}$$

$$
\begin{aligned}
&- f_{\gamma 2}(1 - f_{\gamma' 1})\delta(\hbar\omega - E_{\gamma' 1\gamma 2})]\}2\overline{\Delta\nu} \\
&+ c_{\alpha\beta}^{\gamma\gamma'}(\theta, \varphi)[f_{\gamma 1}(1 - f_{\gamma' 1})\delta(\hbar\omega - E_{\gamma' 1\gamma 1}) \\
&+ f_{\gamma 2}(1 - f_{\gamma' 2})\delta(\hbar\omega - E_{\gamma' 2\gamma 2})]\delta_{\alpha\beta} \\
&+ d_{\alpha\beta}^{\gamma\gamma'}(\theta, \varphi)[f_{\gamma 1}(1 - f_{\gamma' 2})\delta(\hbar\omega - E_{\gamma' 2\gamma 1}) \\
&+ f_{\gamma 2}(1 - f_{\gamma' 1})\delta(\hbar\omega - E_{\gamma' 1\gamma 2})]\delta_{\alpha\beta}]] \qquad (15)
\end{aligned}
$$

where the quantities $a^{\gamma\gamma'}$, $b^{\gamma\gamma'}$, $c_{\alpha\beta}^{\gamma\gamma'}$ and $d_{\alpha\beta}^{\gamma\gamma'}$ are of the order of $(\bar{h}_{so}/\bar{E}_{\lambda\lambda'})^2$. hence the symmetric tensor component can be represented as a sum of two contributions. One of them has peculiarities at the same frequencies as the antisymmetric component Im $\sigma_{xy}^{a[001]}(\omega)$; the second term of equation (15) has a sharp structure at those frequencies corresponding to the electron spin-flip transitions. It should be noted that the diagonal tensor component has a non-vanishing contribution in the small-magnetization limit in contrast to the non-diagonal one. This contribution is due to the crystal anisotropy and is not related to the exchange splitting.

The transitions of the spin-flip type can possess information about the exchange splitting of the electron states.

4. Relations with the phenomenology

One of the most observable and measurable phenomena immediately related with the conductivity tensor components is the magneto-optical Kerr effect in its various configurations. This effect can be briefly clarified in the framework of the reflection problem [12–15]. To describe the reflection problem, some vectors should be introduced: the normal to the sample surface unit vector $\boldsymbol{q}$, the normal to the light incidence plane vector $\boldsymbol{s}$ ($s = \sin\gamma$, γ is the angle between the propagation direction and vector $\boldsymbol{q}$), the complex propagation vector $\boldsymbol{n}$, which can be represented as a sum $(\boldsymbol{q} \times \boldsymbol{s}) + g\boldsymbol{q}$, where $n^2 = g^2 + s^2$, and magnetization unit vector $\boldsymbol{b}$. The mutual position of these vectors determines the usual Kerr effect configurations: (i) *normal-incidence Kerr effect with* $\boldsymbol{b} = \boldsymbol{q}$, when the propagation vector $\boldsymbol{n}$ is inclined along the magnetization direction; (ii) equatorial Kerr effect configuration (the case of propagation perpendicular to the direction of magnetization) with $\boldsymbol{b} = \boldsymbol{s}/s$; and (iii) longitudinal Kerr effect configuration with $\boldsymbol{b} = (\boldsymbol{q} \times \boldsymbol{s})/s$.

As is known, the relations between the electric vector amplitudes A_s, A_p of the incident light and R_s, R_p of the wave reflected from ferromagnets are described by the reflectivity matrix $\hat{r}$:

$$
\begin{pmatrix} R_s \\ R_p \end{pmatrix} = \begin{pmatrix} r_{ss} & r_{sp} \\ r_{ps} & r_{pp} \end{pmatrix} \begin{pmatrix} A_s \\ A_p \end{pmatrix}
$$

where s and p denote the components that are normal and parallel to the incident plane, respectively. If the conductivity tensor is supposed to be a sum of isotropic $\hat{\sigma}_0$ and anisotropic $\hat{\kappa}$ parts, then obvious relations between the reflectivity matrix and conductivity tensor components can be extracted from Maxwell's equations and corresponding boundary conditions [16]. In accordance with these relations, the anisotropic effects lead to the corrections of the reflectivity matrix components r_{ss}, r_{sp}, r_{ps} and r_{pp} expressed in terms of κ_{ss}, κ_{sp}, $\kappa_{p's}$ and $\kappa_{p'p}$, respectively. The quantities κ_{ij} denote the

components of the tensor $\hat{\kappa}$ in the reference frame based on the vectors s, $p = (n_0 \times s)/n_0$ and $p' = (n_0' \times s)/n_0$:

$$\kappa_{ij} = (1/ij)\hat{i}\hat{\kappa}\hat{j} \qquad i,j = s,p,p' \tag{16}$$

where $n_0 = (q \times s) + g_0 q$ is the refracted wave propagation vector, and $n_0' = (q \times s) - g_0 q$ is the vector obtained from the vector n_0 by the mirror operation in the sample surface plane. Then for the reflected linearly polarized s (p) waves, the effects of the reflected light intensity change due to the magnetic anisotropy are expressed by the corrections δr to r_{ii} discussed above:

$$\delta_i = 2\,\mathrm{Re}(\delta r_{ii}/r_{ii}^0) \qquad i = s,p \tag{17}$$

and the effects of the light polarization change (Kerr rotation angle α_K and ellipticity β_K) are expressed by the non-diagonal terms:

$$\alpha_s = \mathrm{Re}(r_{ps}/r_{ss}^0) \quad \alpha_p = -\mathrm{Re}(r_{sp}/r_{pp}^0) \quad \beta_s = \mathrm{Im}(r_{ps}/r_{ss}^0) \quad \beta_p = -\mathrm{Im}(r_{sp}/r_{pp}^0) \tag{18}$$

where r_{ii}^0 are referred to the non-magnetic phase of the crystal:

$$r_{ss}^0 = (\cos\gamma - g_0)/(\cos\gamma + g_0) \qquad r_{pp}^0 = (n_0^2\cos\gamma - g_0)/(n_0^2\cos\gamma + g_0).$$

The quantities that are usually measured in experiments are $\delta_{s(p)}$, $\alpha_{s(p)}$ and $\beta_{s(p)}$. As shown by Krinchik *et al* [13, 17], there are quadratic in M magneto-optical reflection effects, which can be described by the difference of the light intensity change $\delta_{s(p)}$ between equatorial and longitudinal Kerr configurations, i.e. by $\delta_{s(p)}^{equat} - \delta_{s(p)}^{mer}$. The relations between orientation magneto-optical effect (OMOE) $(\delta_{s(p)}^{equat} - \delta_{s(p)}^{mer})$ and the dielectric tensor components can be presented as follows (for the case of linearly p-polarized incident light):

$$\delta_p^{equat} - \delta_p^{mer} = -2\cos\gamma\,\mathrm{Re}\,\frac{\varepsilon(\kappa_{p'p}^{b\|s} - \kappa_{p'p}^{b\|(q\times s)})}{(\varepsilon-1)(\varepsilon\cos^2\gamma - \sin^2\gamma)(\varepsilon - \sin^2\gamma)^{1/2}} \tag{19}$$

where $\varepsilon(\omega)$ is the isotropic part of the dielectric tensor. In order to get more obvious relations between OMOE and dielectric tensor components and to allow comparison with experiment, it will be useful to write equation (19) for some usual configurations in detail.

(i) OMOE for the surface plane (0 0 1), corresponding to turning of b from [1 0 0] to [0 1 0] directions:

$$\kappa_{p'p}^{[100]} - \kappa_{p'p}^{[010]} = (\varepsilon_{yy}^{[100]} - \varepsilon_{xx}^{[100]})(\varepsilon - \sin^2\gamma)/\varepsilon. \tag{20}$$

Here the superscript of $\varepsilon_{\alpha\beta}$ denotes the magnetization direction, at which the dielectric tensor has the form

$$\hat{\varepsilon}^{[100]} = \begin{pmatrix} \varepsilon_{xx} & 0 & 0 \\ 0 & \varepsilon_{yy} & \varepsilon_{xy} \\ 0 & -\varepsilon_{xy} & \varepsilon_{yy} \end{pmatrix}. \tag{21}$$

(ii) OMOE for the surface plane (0 0 1), corresponding to turning of b from [1 1 0] to $[\bar{1}\,1\,0]$ directions:

$$\kappa_{p'p}^{[110]} - \kappa^{[\bar{1}10]}_{p'p} = 2\varepsilon_{xy}^{[110]}(\varepsilon - \sin^2\gamma)/\varepsilon. \tag{22}$$

The dielectric tensor has the following form for $b\|[1\,1\,0]$:

$$\hat{\varepsilon}^{[110]} = \begin{pmatrix} \varepsilon_{xx} & \varepsilon_{xy} & \varepsilon_{xz} \\ \varepsilon_{xy} & \varepsilon_{xx} & -\varepsilon_{xz} \\ -\varepsilon_{xz} & \varepsilon_{xz} & \varepsilon_{zz} \end{pmatrix}. \tag{23}$$

(iii) OMOE for the surface plane (1 1 0), corresponding to turning of $\boldsymbol{b}$ from [1 1 0] to [0 0 1] directions:

$$\kappa_{p'p}^{[1\bar{1}0]} - \kappa_{p'p}^{[001]} = (\varepsilon_{zz}^{[110]} - \varepsilon_{xx}^{[110]})(\varepsilon - 2\sin^2\gamma)/[\varepsilon(\varepsilon - \sin^2\gamma)]. \tag{24}$$

The presented general form of the dielectric tensor at a given magnetization direction with respect to the crystallographic axes has been easily obtained by the symmetric restrictions imposed by the Laue group of a corresponding magnetic space group [8, 18].

At this point it is trivial to consider the frequency dependence of the even in $\boldsymbol{M}$ part of OMOE. For example, OMOE corresponding to the configurations (i) and (iii) is described by the difference between diagonal components of a dielectric tensor in accordance with equations (20) and (24), and in the case (ii) OMOE is described by the symmetric non-diagonal tensor component in accordance with equation (22). Hence the even in $\boldsymbol{M}$ effect in question has a similar frequency dependence as hand-made corrections to the conductivity tensor perturbatively obtained earlier at second order in SO coupling (equation (12) in general or equations (14) and (15) for the small-magnetization limit). So the main interest in the frequency behaviour of OMOE consists of the peculiarities which are immediately related with the electron spin-flip transitions.

5. Numerical LSDA calculations: application to nickel

The numerical calculations were carried out on the basis of equation (3) for the dissipative parts of the conductivity tensor $\sigma_{\alpha\beta}(\omega)$); then the dispersive parts of the tensor are obtained from the Kramers–Kronig dispersive relations. In a recent paper [8] a detailed analysis of the frequency dependence has been presented for diagonal and odd in $\boldsymbol{M}$ non-diagonal tensor components. So this section is devoted to the frequency behaviour of the even in $\boldsymbol{M}$ magneto-optical Kerr effects. To evaluate the frequency-dependent OMOE expressions (19) for three configurations of the mutual arrangement of the incident light polarization plane and magnetization orientation discussed in the previous section, the band states, one-electron wavefunctions, momentum matrix elements and finally the conductivity tensor components (21) and (23) have been calculated at $\boldsymbol{M}\|[0\,0\,1]$ and $\boldsymbol{M}\|[1\,1\,0]$. The integration over $\boldsymbol{k}$ in equation (3) has been performed by the tetrahedron method with 918 points in the 1/16th irreducible part of the Brillouin zone (IBZ) of $\boldsymbol{M}\|[0\,0\,1]$ and 1836 points in the 1/8th IBZ at $\boldsymbol{M}\|[1\,1\,0]$. It was assumed that such a $\boldsymbol{k}$ mesh is fine enough to get high accuracy at the light frequencies $\hbar\omega \gg \bar{h}_{so}$ but it seems to be rough at $\hbar\omega \sim \bar{h}_{so}$, when about 50000 points are needed to get suitable accuracy [8]. Because of the SO hybridization effects between states with opposite spin projections, the perturbative expressions [11, 12] can be considered as suitable only at $\hbar\omega \gg \bar{h}_{so}$.

The frequency dependence of OMOE at light energies $0 < \hbar\omega < 1.5$ eV are plotted on figure 1. In this range the calculated curves have a sharp peculiarity at $\hbar\omega \sim 0.6$ eV. According to the perturbative analysis presented above, this peculiarity can be considered as a result of the spin-flip transitions, which seem to occur at the d-band exchange splitting energy. In contrast to the prediction presented in [14] there is significant even

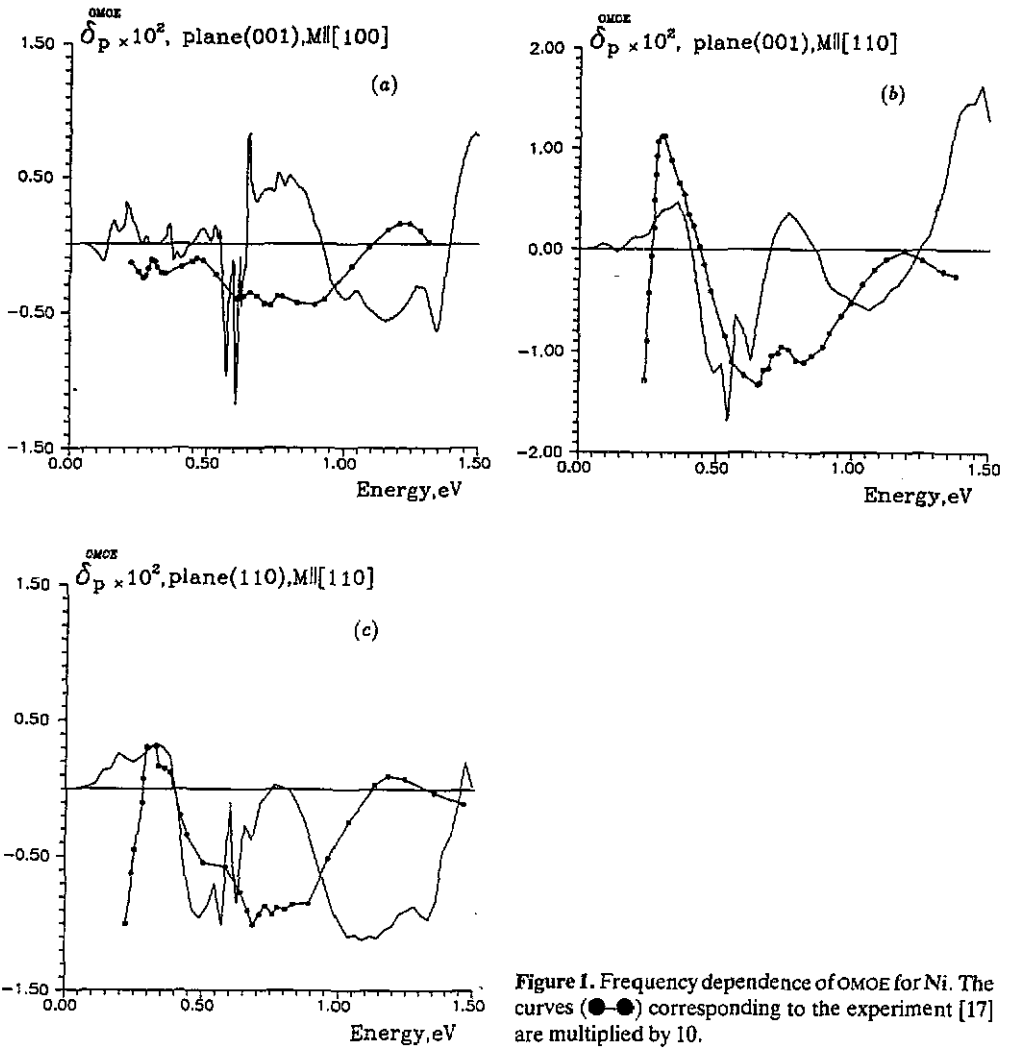

Figure 1. Frequency dependence of OMOE for Ni. The curves (●–●) corresponding to the experiment [17] are multiplied by 10.

in M effect in the plane (0 0 1) and $M \| [1\,0\,0]$ with the same order of magnitude as in other configurations. It should be noted that there are more distinctions between calculated quantities and experimental ones than agreements. Numerical data corresponding to absolute zero exceed the experimental one obtained at $T = 80$ K by nearly one order of magnitude. *It is evident that the calculated curves at* $\hbar\omega > 0.8$ eV *should be compressed* on the energy scale to improve agreement with the frequency behaviour of the experimental curves. It is well known that such 'compression' is needed for whole LSDA valence states with width exceeding the experimental one by nearly 40%. Experimental curves have two main peculiarities at $\hbar\omega \sim 0.3$ eV and ~ 0.6 eV. The peculiarity at $\hbar\omega \sim 0.3$ eV is typical for both diagonal and non-diagonal tensor components and its origin seems to be related with the interband transitions in those regions of k-space where the non-relativistic opposite spin projection bands crossing, as discussed in [8]. Probably the experimental peculiarity that corresponds to the spin-flip transitions occurs at $\hbar\omega \sim 0.6$ eV.

Such disagreement between theory and experiment is rather a proof of the well known LSDA failure in the one-particle treatment of the properties of nickel (see e.g. [8]). One can hope that this failure for Ni is an exception rather than the rule. The results of similar investigations for Fe and Co will be presented elsewhere.

6. Conclusions

In the first and second order in SO coupling we have perturbatively investigated the frequency dependence of both the odd and even in $\boldsymbol{M}$ components of the conductivity tensor for arbitrary orientations of the magnetization vector with respect to the crystallographic axes. The results of significant importance are the frequency peculiarities of the tensor symmetric components, which can be considered as a manifestation of the spin-flip transitions and can possess information about exchange splitting. For comparison with experimental data the corresponding numerical LSDA calculations have been carried out for the orientation magneto-optical Kerr effect at various light polarization and $\boldsymbol{M}$ configurations. The application of analytical and numerical treatments to Ni shows how the magnitude of exchange splitting can be extracted from the corresponding experimental data. Such an approach allows one to get detailed information about the main electron characteristics from the frequency and $\boldsymbol{M}$ orientation dependence of the conductivity tensor components in magnetic metals and compounds.

Acknowledgment

The author would like to thank Dr E A Gan'shina for useful discussions of the experimental data.

Appendix

Substituting equations (8) into (3) and keeping the terms of order $(\bar{h}_{so}/\bar{E}_{\lambda\lambda'})^2$, the following expressions for the factors $A^{\gamma\gamma',\sigma}_{\alpha\beta}(k,\theta,\varphi)$ and $B^{\gamma\gamma',\sigma}_{\alpha\beta}(k,\theta,\varphi)$ can be obtained after some symmetrical restrictions:

(i) For $\alpha \neq \beta$

$$A^{\gamma\gamma',\sigma}_{\alpha\beta}(k,\theta,\varphi) \equiv \sin(2\varphi)\sin^2\theta$$

$$\times \sum_{mm'}{}' \left[L^{m\gamma,m'\gamma'}_{\alpha\beta} P^{mm',\gamma'\gamma}_{\alpha\beta} \left(\frac{1}{E_{\gamma\sigma,m\bar{\sigma}} E_{\gamma'\sigma,m'\bar{\sigma}}} - \frac{1}{E_{\gamma\sigma,m\sigma} E_{\gamma'\sigma,m'\sigma}} \right) \right.$$

$$+ L^{mm',m'\gamma}_{\alpha\beta} P^{m\gamma',\gamma'\gamma}_{\alpha\beta} \left(\frac{1}{E_{\gamma\sigma,m'\sigma} E_{\gamma\sigma,m\sigma}} - \frac{1}{E_{\gamma\sigma,m'\bar{\sigma}} E_{\gamma\sigma,m\sigma}} \right)$$

$$+ L^{m'm,m\gamma'}_{\alpha\beta} P^{\gamma m',\gamma'\gamma}_{\alpha\beta} \left(\frac{1}{E_{\gamma'\sigma,m\sigma} E_{\gamma'\sigma,m'\sigma}} - \frac{1}{E_{\gamma'\sigma,m\bar{\sigma}} E_{\gamma'\sigma,m'\sigma}} \right)$$

$$\left. + L^{m\gamma,m\gamma}_{\alpha\beta} P^{\gamma\gamma',\gamma'\gamma}_{\alpha\beta} \left(\frac{1}{E^2_{\gamma\sigma,m\bar{\sigma}}} - \frac{1}{E^2_{\gamma\sigma,m\sigma}} \right) \delta_{mm'} \right.$$

$$+ L_{\alpha\beta}^{m\gamma,m\gamma'} P_{\alpha\beta}^{\gamma\gamma',\gamma'\gamma} \left(\frac{1}{E_{\gamma'\sigma,m\bar{\sigma}}^2} - \frac{1}{E_{\gamma'\sigma,m\sigma}^2} \right) \delta_{mm'}$$

$$+ L_{\alpha\beta}^{m\gamma,m'\gamma'} P_{\alpha\beta}^{m\gamma',m'\gamma} \frac{1}{E_{\gamma\sigma,m\sigma} E_{\gamma'\sigma,m'\sigma}}$$

$$- L_{\alpha\beta}^{m\gamma,m'\gamma} P_{\alpha\beta}^{m\gamma',\gamma'm} \frac{1}{2E_{\gamma\sigma,m\sigma} E_{\gamma\sigma,m'\sigma}} - L_{\alpha\beta}^{m'\gamma',m\gamma'} P_{\alpha\beta}^{\gamma m',m\gamma} \frac{1}{2E_{\gamma'\sigma,m'\sigma} E_{\gamma'\sigma,m\sigma}} \Bigg]$$

$$B_{\alpha\beta}^{\gamma\gamma',\sigma}(\boldsymbol{k}, \theta, \varphi) \equiv \sin(2\varphi) \sin^2 \theta \sum_{mm'}{}' \left(-L_{\alpha\beta}^{m\gamma,m'\gamma'} P_{\alpha\beta}^{m\gamma',m'\gamma} \frac{1}{E_{\gamma\sigma,m\bar{\sigma}} E_{\gamma'\bar{\sigma},m'\sigma}} \right.$$

$$+ L_{\alpha\beta}^{m\gamma,m'\gamma} P_{\alpha\beta}^{m\gamma',\gamma'm} \frac{1}{2E_{\gamma\bar{\sigma},m\sigma} E_{\gamma\bar{\sigma},m'\sigma}}$$

$$\left. + L_{\alpha\beta}^{m'\gamma',m\gamma'} P_{\alpha\beta}^{\gamma m',m\gamma} \frac{1}{2E_{\gamma'\bar{\sigma},m'\sigma} E_{\gamma'\bar{\sigma},m\sigma}} \right).$$

(ii) For $\alpha = \beta$

$$A_{\alpha\alpha}^{\gamma\gamma',\sigma}(\boldsymbol{k}, \theta, \varphi) \equiv \sum_{mm'}{}' \left\{ \left[L^{m\gamma,m'\gamma'}(\theta, \varphi) \left(\frac{1}{E_{\gamma\sigma,m\bar{\sigma}} E_{\gamma'\sigma,m'\bar{\sigma}}} - \frac{1}{E_{\gamma\sigma,m\sigma} E_{\gamma'\sigma,m'\sigma}} \right) \right.\right.$$

$$\left. - Sp\mathcal{L}^{m\gamma,m'\gamma'} \frac{1}{E_{\gamma\sigma,m\bar{\sigma}} E_{\gamma'\sigma,m'\bar{\sigma}}} \right] P_{\alpha\alpha}^{mm',\gamma'\gamma}$$

$$+ \left[L^{mm',m'\gamma}(\theta, \varphi) \left(\frac{1}{E_{\gamma\sigma,m'\sigma} E_{\gamma\sigma,m\sigma}} - \frac{1}{E_{\gamma\sigma,m'\bar{\sigma}} E_{\gamma\sigma,m\sigma}} \right) \right.$$

$$\left. + Sp\mathcal{L}^{mm',m'\gamma} \frac{1}{E_{\gamma\sigma,m'\bar{\sigma}} E_{\gamma\sigma,m\sigma}} \right] P_{\alpha\alpha}^{m\gamma',\gamma'\gamma}$$

$$+ \left[L^{m'm,m\gamma'}(\theta, \varphi) \left(\frac{1}{E_{\gamma'\sigma,m\sigma} E_{\gamma'\sigma,m'\sigma}} - \frac{1}{E_{\gamma'\sigma,m\bar{\sigma}} E_{\gamma'\sigma,m'\sigma}} \right) \right.$$

$$\left. + Sp\mathcal{L}^{m'm,m\gamma'} \frac{1}{E_{\gamma'\sigma,m\bar{\sigma}} E_{\gamma'\sigma,m'\sigma}} \right] P_{\alpha\alpha}^{\gamma m',\gamma'\gamma}$$

$$+ \tfrac{1}{2} \left[L^{m\gamma,m\gamma}(\theta, \varphi) \left(\frac{1}{E_{\gamma\sigma,m\sigma}^2} - \frac{1}{E_{\gamma\sigma,m\bar{\sigma}}^2} \right) + \frac{Sp\mathcal{L}^{m\gamma,m\gamma}}{E_{\gamma\sigma,m\bar{\sigma}}^2} \right] \delta_{mm'} P_{\alpha\alpha}^{\gamma\gamma',\gamma'\gamma}$$

$$+ \tfrac{1}{2} \left[L^{m\gamma',m\gamma'}(\theta, \varphi) \left(\frac{1}{E_{\gamma'\sigma,m\sigma}^2} - \frac{1}{E_{\gamma'\sigma,m\bar{\sigma}}^2} \right) + \frac{Sp\mathcal{L}^{m\gamma',m\gamma'}}{E_{\gamma'\sigma',m\bar{\sigma}}^2} \right] \delta_{mm'} P_{\alpha\alpha}^{\gamma\gamma',\gamma'\gamma}$$

$$+ L^{m\gamma,m'\gamma'}(\theta, \varphi) P_{\alpha\alpha}^{m\gamma',m'\gamma} \frac{1}{E_{\gamma\sigma,m\sigma} E_{\gamma'\sigma,m'\sigma}}$$

$$- L^{m\gamma,m'\gamma}(\theta, \varphi) P_{\alpha m}^{m\gamma',\gamma'm} \frac{1}{2E_{\gamma\sigma,m\sigma} E_{\gamma\sigma,m'\sigma}}$$

$$\left. - L^{m'\gamma',m\gamma'}(\theta, \varphi) P_{\alpha\alpha}^{\gamma m',m\gamma} \frac{1}{2E_{\gamma'\sigma,m'\sigma} E_{\gamma'\sigma,m\sigma}} \right\}$$

and

$$B^{\gamma\gamma',\sigma}_{\alpha\alpha'}(k,\theta,\varphi) \equiv \sum_{mm'}{}' \left((Sp\mathcal{L}^{m\gamma,m'\gamma'} - L^{m\gamma,m'\gamma'}) \frac{1}{E_{\gamma\sigma,m\bar{\sigma}} E_{\gamma'\bar{\sigma},m'\sigma}} P^{m\gamma',m'\gamma}_{\alpha\alpha'} \right.$$

$$- (Sp\mathcal{L}^{m\gamma,m'\gamma} - L^{m\gamma,m'\gamma}) \frac{1}{2E_{\gamma\bar{\sigma},m\sigma} E_{\gamma\bar{\sigma},m'\sigma}} P^{m\gamma',\gamma'm}_{\alpha\alpha'}$$

$$\left. - (Sp\mathcal{L}^{m'\gamma',m\gamma'} - L^{m'\gamma',m\gamma'}) \frac{1}{2E_{\gamma'\bar{\sigma},m'\sigma} E_{\gamma'\bar{\sigma},m\sigma}} P^{\gamma m',m\gamma}_{\alpha\alpha'} \right).$$

Here $\sigma(\bar{\sigma}) = 1(2), 2(1)$ are the spin indices, the matrix elements for the non-diagonal tensor components are

$$L^{m\gamma,m'\gamma'}_{xy} \equiv \langle \xi l_x \rangle_{m\gamma} \langle \xi l_y \rangle_{m'\gamma'} + \langle \xi l_y \rangle_{m\gamma} \langle \xi l_x \rangle_{m'\gamma'}$$

$$P^{m\gamma,m'\gamma}_{xy} \equiv p^{m\gamma}_x p^{m'\gamma}_y + p^{m\gamma}_y p^{m'\gamma}_x$$

and for the diagonal components

$$L^{m\gamma,m'\gamma'}(\theta,\varphi) \equiv L^{m\gamma,m'\gamma'}_{xx} \cos^2\varphi \sin^2\theta + L^{m\gamma,m'\gamma'}_{yy} \sin^2\varphi \sin^2\theta + L^{m\gamma,m'\gamma'}_{zz} \cos^2\theta$$

$$Sp\mathcal{L}^{m\gamma,m'\gamma'} \equiv L^{m\gamma,m'\gamma'}_{xx} + L^{m\gamma,m'\gamma'}_{yy} + L^{m\gamma,m'\gamma'}_{zz}.$$

The second term presenting the SO contribution to the momentum operator in expression (4) has been omitted in obtaining the perturbative expressions. It is quite justified by the obvious smallness of the ratio between the mentioned term and the term that arises due to the first order in SO perturbative correction to the wavefunction, which can roughly be estimated $(\bar{E}_{\lambda\lambda'}/4mc^2)(\bar{E}_{\lambda\lambda'}/\bar{h}_{so}) \sim 10^{-5}$. Even in comparison with the term that arises due to the second order in SO perturbative contribution to the wavefunction, the term in question is as small as $(\bar{E}_{\lambda\lambda'}/4mc^2)(\bar{E}_{\lambda\lambda'}/\bar{h}_{so})^2 \sim 10^{-4}$. This is justified by the numerical calculations also.

References

[1] Daalderop G H, Kelly P J and Schuurmans M F H 1990 *Phys. Rev.* B **42** 1533
[2] Chun Li, Freeman A J, Jansen H J F and Fu C L 1990 *Phys. Rev.* B **42** 5433
[3] Landau L V and Lifshitz E M 1974 *Electrodynamics* (Moscow: Nauka)
[4] Argyres P N 1955 *Phys. Rev.* **97** 334
[5] Kubo R 1957 *J. Phys. Soc. Japan* **12** 570
[6] Kübler J, Höck K-H, Sticht J and Williams A R 1988 *J. Phys. F: Met. Phys.* **18** 469
[7] Andersen O K 1975 *Phys. Rev.* B **12** 3060
[8] Halilov S V and Uspenskii Yu A 1990 *J. Phys.: Condens. Matter* **2** 6137
[9] Feder R, Rosicky F and Ackerman B 1983 *Z. Phys.* B **52** 31
[10] Strange P, Staunton J and Gyorffy B L 1984 *J. Phys. C: Solid State Phys.* **17** 3355
[11] Cortona P, Doniach S and Sommers C 1985 *Phys. Rev.* A **31** 2842
[12] Bolotin G A and Sokolov A V 1961 *Fiz. Metall. Metalloved.* **12** 785
[13] Krinchik G S and Guschin V S 1969 *JETP Lett.* **10** 35
[14] Donovan B and Webster J 1962 *Proc. Phys. Soc.* **79** 46
[15] Webster J and Donovan B 1965 *Br. J. Appl. Phys.* **16** 25
[16] Bolotin G A 1975 *Fiz. Metall. Metalloved.* **39** 731
[17] Krinchik G S and Gan'shina E A 1973 *Sov. Phys.–JETP* **65** 1970
[18] Kleiner W H 1966 *Phys. Rev.* **142** 318